Icarus 210 (2010) 480–487

Contents lists available at ScienceDirect

Icarus

journal homepage: www.elsevier.com/locate/icarus

The formation and stability of carbonic acid on outer Solar System bodies

Z. Peeters [a,b], R.L. Hudson [a,c,*], M.H. Moore [a], Ariel Lewis [c]

[a] Code 691, NASA Goddard Space Flight Center, Greenbelt, MD 20771, United States
[b] Department of Chemistry, The Catholic University of America, Washington, DC 20064, United States
[c] Department of Chemistry, Eckerd College, St. Petersburg, FL 33711, United States

ARTICLE INFO

Article history:
Received 2 July 2009
Revised 28 May 2010
Accepted 2 June 2010
Available online 9 June 2010

Keywords:
Ices, IR spectroscopy
Satellites, Surfaces
Cosmic rays

ABSTRACT

The radiation chemistry, thermal stability, and vapor pressure of solid-phase carbonic acid (H_2CO_3) have been studied with mid-infrared spectroscopy. A new procedure for measuring this molecule's radiation stability has been used to obtain intrinsic IR band strengths and half-lives for radiolytic destruction. We report, for the first time, measurements of carbonic acid's vapor pressure ($0.290–2.33 \times 10^{-11}$ bar for 240–255 K) and its enthalpy of sublimation (71 ± 9 kJ mol^{-1}). We also report the first observation of a chemical reaction involving solid-phase carbonic acid. Possible applications of these findings are discussed, with an emphasis on the outer Solar System icy surfaces.

Published by Elsevier Inc.

1. Introduction

The general impression one gains in reading the literature, including many chemistry texts, is that carbonic acid (H_2CO_3) is an unstable molecule with a fleeting existence. While this impression is warranted at physiological temperatures (~37 °C), it is inaccurate at temperatures found in the outer Solar System and in interstellar space. Laboratory experiments from nearly 20 years ago (Moore and Khanna, 1991; Moore et al., 1991) showed that H_2CO_3 is formed by ion-irradiation of $H_2O + CO_2$ mixtures at ~20 K followed by warming to remove residual reactants and volatile products. This H_2CO_3 identification was confirmed by similar experiments with $H_2O + CO_2$ ices using vacuum-ultraviolet photons (Gerakines et al., 2000; Wu et al., 2003) and 5–10 keV electrons (Hand et al., 2007; Zheng and Kaiser, 2007). Other studies revealed that H^+ implantation into frozen CO_2 and $H_2O + CO_2$ mixtures also results in carbonic acid formation (Brucato et al., 1997). All authors agree that H_2CO_3 is a major product of low-temperature $H_2O + CO_2$ photo- and radiation chemistry, with minor products including H_2O_2, CO, O_3, and CO_3.

Combining all of the earlier work, it can be concluded that H_2O, CO_2, and an eV-to-MeV energy source are all that is needed to make and trap H_2CO_3, provided the temperature is kept below about 250 K. These conditions can be found at multiple locations in the outer Solar System. Both H_2O and CO_2 have been observed on the jovian satellites Europa (Hansen and McCord, 2008), Ganymede (Hibbitts et al., 2003), and Callisto (Hibbitts et al., 2000); Saturn's satellites Enceladus, Dione, Hyperion, Iapetus, and Phoebe (Brown et al., 2006; Filacchione, 2007; Clark et al., 2008); the uranian satellites Ariel, Umbria, and Titania (Grundy et al., 2006); and Neptune's satellite Triton (Grundy and Young, 2004). Each of these surfaces is exposed to the radiation environment of the closest planet. In each case, carbonic acid may be formed, and for Callisto a tentative detection of H_2CO_3 already has been made (Johnson et al., 2004).

To assess the formation and stability of carbonic acid in the Solar System, it is important to investigate the molecule's physical and chemical properties, but little such work has been published to date. Gerakines et al. (2000) compared the yields of H_2CO_3 made by exposing $H_2O + CO_2$ ice mixtures to ion-irradiation (~1 MeV H^+) and to UV photons (~10 eV). The same researchers measured carbonic acid's intrinsic IR band strengths by the growth of products resulting from UV destruction of H_2CO_3. Earlier work also showed qualitatively that carbonic acid's vapor pressure is lower than that of H_2O, CO_2, and the observed reaction products, since H_2CO_3 is the last of these to sublime under vacuum in the 200–250 K region (Moore and Khanna, 1991). A white color is likely for H_2CO_3 made by acid–base chemistry (photographs in Loerting et al., 2000), and the work by Winkel et al. (2007) showed that the X-ray powder pattern of frozen H_2CO_3 is featureless.

In this paper, we reinvestigate the intrinsic IR band strengths of H_2CO_3 and, for the first time, measure this molecule's radiolytic destruction at several temperatures. These new radiation experiments take into account amorphization of the sample. Furthermore, the highest temperature at which destruction measurements are made has been raised from ~10 K to 200 K. Temperature-dependent changes in the position and width of the H_2CO_3 feature at 2618 cm^{-1} (3.82 μm) have been recorded. The first

* Corresponding author at: Code 691, NASA Goddard Space Flight Center, Greenbelt, MD 20771, United States. Fax: +1 301 286 0440.
E-mail address: Reggie.Hudson@NASA.gov (R.L. Hudson).

0019-1035/$ - see front matter Published by Elsevier Inc.
doi:10.1016/j.icarus.2010.06.002

measurements of the vapor pressure and heat of vaporization of pure H_2CO_3 are given, along with the first example of a low-temperature acid–base reaction of the molecule.

2. Experimental

In each experiment described in this paper, carbonic acid first was made either by ion-irradiation of an $H_2O + CO_2$ ice or by a low-temperature acid–base reaction between HBr and $KHCO_3$, followed by warming the resulting mixture under vacuum, effectively freeze-drying and purifying the H_2CO_3. Both synthetic methods will be described. Many of the other details concerning our experimental setup, and procedures for growing and ion-irradiating ice films, were presented in earlier papers (e.g., Moore et al., 2007; Hudson and Moore, 2004).

An initial gas mixture was made by combining equal partial pressures of water vapor (from 18 MΩ cm H_2O) and CO_2 (Matheson, research grade) or $^{13}CO_2$ (Cambridge Isotopes, 99%). This mixture was led through a metering valve into a high-vacuum chamber ($\sim 10^{-7}$ torr) and then condensed onto a pre-cooled (~14 K) aluminum mirror connected to a closed-cycle helium cryostat. A typical ice film had a thickness of ~5 μm and an area of ~5 cm^2. Such films were irradiated with 0.8 MeV protons from a Van de Graaff accelerator to a fluence of about 1×10^{15} protons cm^{-2} (current ~0.1 μA). Doses were calculated as described in Moore and Hudson (1998) using the average stopping power and molecular density of the ice (Table 1), and the measured proton fluence. All radiation doses were converted to a common scale of eV per 16-amu molecule, referred to as simply "eV per molecule" in the remainder of this paper. The eV per 16-amu scale was chosen so that our results could be compared directly to published data. Irradiated samples were warmed to 240 K to sublime away the unreacted H_2O and CO_2, as well as the reaction products, leaving a layer of pure crystalline H_2CO_3.

Changes in the IR spectra of irradiated ices were followed by Fourier-transform infrared (FTIR) spectroscopy using a Nicolet Nexus 670 instrument. In this setup, the incident IR beam passed through the sample, was reflected by the underlying aluminum mirror, and then passed through the ice a second time, and to the IR detector, for what are sometimes called transmission–reflection–transmission spectra. Measurements were made at 2 cm^{-1} resolution from 5000 to 650 cm^{-1}, averaged over 150 scans.

For studying the vapor pressure of H_2CO_3, the compound first was made by an acid–base reaction between a 1 M solution of HBr (Sigma–Aldrich) and a 0.1 M solution of $KHCO_3$ (Sigma–Aldrich), similar to the technique of Hage et al. (1993). A few microliters of the $KHCO_3$ solution were injected through a septum, using a syringe, onto a KBr substrate at 10 K, attached to the tail section of a closed-cycle helium cryostat. Next, a few microliters of the HBr solution were injected the same way to form a layer atop the frozen $KHCO_3$ solution. This process was repeated about 10 times to increase the ice's thickness. Subsequent warming of the sample to ~200 K removed the H_2O and initiated a reaction between HBr and $KHCO_3$ to form H_2CO_3, with spectral changes that were followed with IR spectroscopy. The sample then was heated to 240–255 K, and IR spectra recorded over time, with a focus on the 1300 and 1500 cm^{-1} features of H_2CO_3. Band areas were measured and combined with intrinsic band strengths, so called *A* values, to determine the vapor pressures and enthalpy of sublimation (ΔH_{sub}) of H_2CO_3 (Khanna et al., 1990). These measurements were made with a Mattson Polaris spectrometer operating in a conventional transmission mode.

Table 1
Physical properties of ices.

Ice	Molecular mass (g mol^{-1})	Density (g cm^{-3})	Proton stopping power[c] (MeV cm^2 g^{-1})
H_2O	18	1	273
CO_2	44	1.7	240
$H_2O + CO_2$ (1:1)	31	1.35[a]	256.5[a]
H_2CO_3	62	1[b]	254

[a] Average value for a $H_2O + CO_2$ (1:1) mixture.
[b] Assumed value.
[c] Calculated for 0.8 MeV protons, according to method of Ziegler et al. (1985).

3. Results

We first present new measurements on the radiolytic destruction of H_2CO_3. These results were used to redetermine the intrinsic band strengths of H_2CO_3, which we then describe. The band strengths, in turn, were critical for calculating the other properties that we report, namely carbonic acid's radiolytic yield (*G* value) and its vapor pressures.

3.1. Spectroscopy

Trace (a) in Fig. 1 shows the mid-IR spectrum of a $H_2O + CO_2$ (1:1) ice mixture at 14 K. Upon irradiation of the ice to a dose of 6.8 eV $molec^{-1}$, new features appeared in the spectrum, as seen in trace (b). The new bands at 2580, 1712, 1483, 1294, and 1016 cm^{-1} are assigned to H_2CO_3, while features at 2853, 2143, 2045, and 1038 cm^{-1} are due to H_2O_2, CO, CO_3, and O_3, respectively. Upon warming to 240 K, H_2O, CO_2, and all irradiation products except H_2CO_3 sublimed into the vacuum system. Traces (c) and (d) of Fig. 1 show the resulting spectra of crystalline H_2CO_3 at 240 K, and after recooling to 14 K.

IR peak positions of H_2CO_3 and $H_2{}^{13}CO_3$ at 14, 100, and 200 K are listed in Table 2, with band assignments from Gerakines et al. (2000) and DelloRusso et al. (1993). For the strongest H_2CO_3 band in the 2–5 μm region, at 2618 cm^{-1} (3.820 μm), the position and full-width at half-maximum (FWHM) were measured from 10 to 240 K. The results are shown in Fig. 2.

3.2. Radiolytic destruction

The destruction of crystalline H_2CO_3 by 0.8 MeV protons was followed by measuring the decrease in IR band areas after various

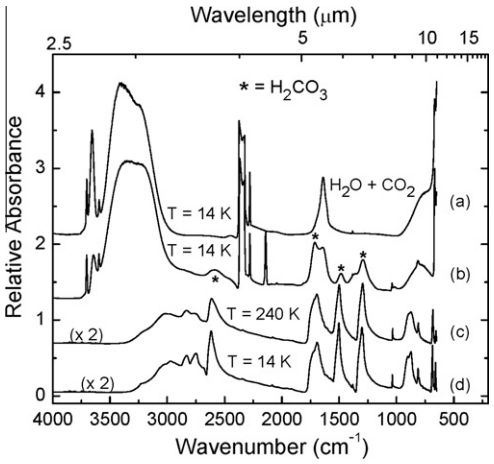

Fig. 1. (a) Infrared spectrum of $H_2O + CO_2$ (1:1) ice at 14 K. (b) The same ice after proton irradiation to a dose of 6.8 eV $molec^{-1}$ shows new features identified with H_2CO_3, and indicated by asterisks. (c) Spectrum of crystalline H_2CO_3 at 240 K after H_2O, CO_2, and minor volatiles sublime. (d) Crystalline H_2CO_3 after recooling from 240 K to 14 K.

Table 2
IR band positions for crystalline $H_2{}^{12}CO_3$ and $H_2{}^{13}CO_3$.

H_2CO_3 band assignment[a]	Band position (cm^{-1})			Integration limits (cm^{-1})
	14 K	100 K	200 K	
H_2CO_3				
O—H stretch	2749 + 2833	2757 + 2833	2764 + 2832	2660–2883
O—H stretch	2618	2618	2615	2450–2660
C=O stretch	1695	1695	1696	1554–1794
C—OH asym. stretch	1503	1503	1501	1385–1554
C—OH i.p. bend	1303	1301	1297	1065–1385
C—OH sym. stretch	1038	1037	1036	1020–1050
C—OH o.p. bend	875	875	875	826–985
$H_2{}^{13}CO_3$				
O—H stretch	2748 + 2813	2756 + 2810	2762 + 2808	2660–2883
O—H stretch	2617	2614	2611	2450–2660
C=O stretch	1662	1662	1662	1554–1794
C—OH asym. stretch	1476	1473	1474	1385–1554
C—OH i.p. bend	1288	1285	1289	1065–1385
C—OH sym. stretch	1037	1036	1035	1020–1050
C—OH o.p. bend	904	899	883	826–985

[a] Assignments are from Gerakines et al. (2000) and DelloRusso et al. (1993). The abbreviations i.p. and o.p. refer to in-plane and out-of-plane vibrations, respectively.

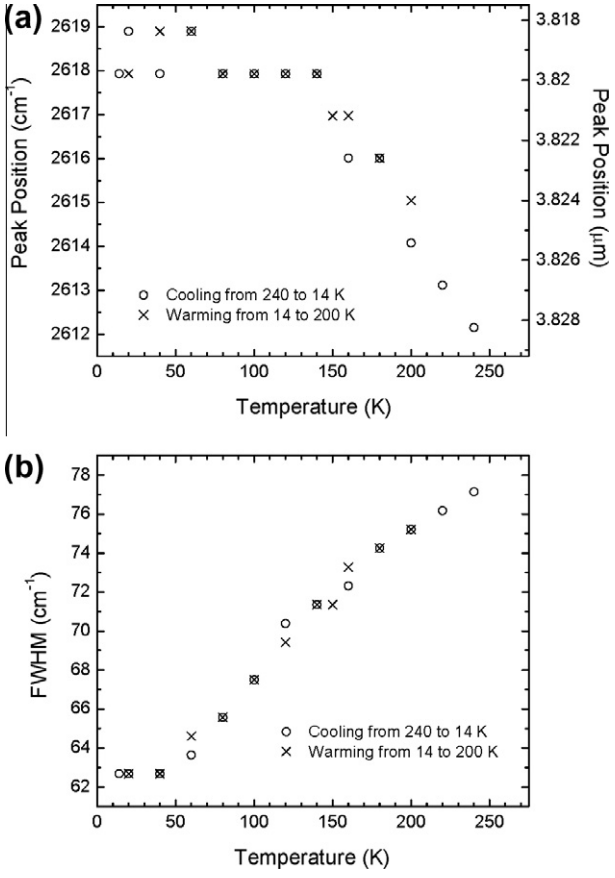

Fig. 2. Peak position and full-width at half-maximum (FWHM) of the 2618 cm^{-1} (3.820 μm) band of crystalline-phase H_2CO_3 as a function of temperature.

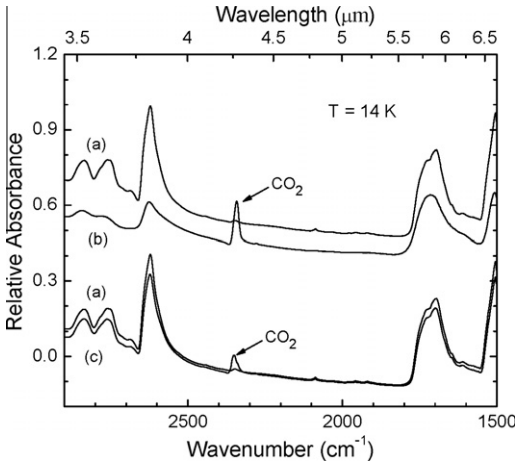

Fig. 3. H_2CO_3 spectra are compared at 14 K between 2900 and 1500 cm^{-1} (a) before and (b) after irradiation to a dose of 5.2 eV $molec^{-1}$, and (c) after warming to 200 K and recooling to 14 K. The irradiated H_2CO_3 shows weaker, broader bands than the unirradiated material. The lower pair of traces compares the (c) annealed sample's spectrum to the (a) original spectrum.

doses. As an example, spectra in the 2900–1500 cm^{-1} (3.45–6.67 μm) region before and after irradiation to a dose of 2.0 eV $molec^{-1}$ are compared in Fig. 3. The H_2CO_3 bands are seen to decrease, indicating a loss of molecules, and at the same time H_2O and CO_2 are formed (H_2O is not shown). In addition, irradiation caused the H_2CO_3 bands to widen, indicating amorphization of the crystalline sample.

To accurately quantify carbonic acid's radiolytic destruction it was necessary to distinguish between spectral changes caused by (a) loss of H_2CO_3 molecules and (b) amorphization. This was done by warming the sample to 200 K after each irradiation step to fully recrystallize the partially-amorphous ice and to sublime away the H_2O and CO_2 formed by radiolysis. The ice then was recooled to 14 K, as shown in trace (c) of Fig. 3, for comparison to the original spectrum of the unirradiated ice, trace (a). Spectra a and c are similar, but the latter has slightly smaller H_2CO_3 bands, caused by the destruction of crystalline H_2CO_3.

The normalized band areas for H_2CO_3 have been plotted in Fig. 4 as a function of radiation dose. Table 2 lists all bands that were averaged for this graph along with their integration limits. Also in Fig. 4 are linear regression lines through the data points. The corresponding half-life doses for H_2CO_3 irradiated at 14, 100, and 200 K are then 11, 11, and 7 eV $molec^{-1}$, respectively.

3.3. Intrinsic band strengths

For our experiments, Eq. (1) is the connection among the column density (N, molec cm^{-2}) of a molecule in an ice sample, the

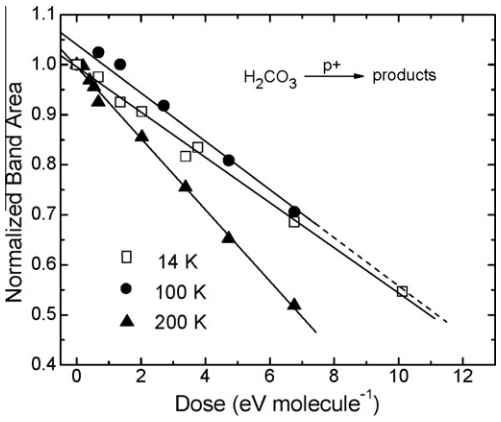

Fig. 4. Normalized band areas of H_2CO_3 as a function of radiation dose at 14, 100, and 200 K. Each point is an average of areas for the spectral bands listed in Table 2. For the 14 and 100 K experiments, the sample was warmed to 200 K after each irradiation step and then recooled to the starting temperature to recrystallize any amorphous ice.

molecule's intrinsic band strength (A, cm molec^{-1}), and the integrated absorbance of a spectral band:

$$N = \frac{\ln 10 \int \mathrm{Abs}(\tilde{\nu})\, d\tilde{\nu}}{2A} \quad (1)$$

The "ln10" coefficient converts from common to natural logarithms and the factor of "2" accounts for the two passes our IR beam makes through an ice, at nearly normal incidence. See also d'Hendecourt and Allamandola (1986).

Eq. (1) was used to determine the A values of H_2CO_3 as follows. Spectra a and b in Fig. 3 show that carbon dioxide is a radiation decomposition product of carbonic acid, with the overall reaction being (2):

$$H_2CO_3 \rightarrow H_2O + CO_2 \quad (2)$$

The 1:1 stoichiometry of (2) requires that any increase in the CO_2 column density of the ice be matched by a loss of H_2CO_3, so that in absolute terms $\Delta N(CO_2) = \Delta N(H_2CO_3)$ for each radiation dose. From this, and relationship (1), Eq. (3) is obtained:

$$\frac{\Delta\left(\int \mathrm{Abs}(\tilde{\nu})\, d\tilde{\nu}\right)_{CO_2}}{A(CO_2)} = \frac{\Delta\left(\int \mathrm{Abs}(\tilde{\nu})\, d\tilde{\nu}\right)_{H_2CO_3}}{A(H_2CO_3)} \quad (3)$$

Values of $A(CO_2)$ are known (Gerakines et al., 1995), and so measurements of CO_2 and H_2CO_3 band areas at different radiation doses allowed calculation of $A(H_2CO_3)$ from Eq. (3).

For our determinations of $A(H_2CO_3)$, we proton-irradiated H_2CO_3 to form CO_2. After each radiation step, the changes in the CO_2 and H_2CO_3 band areas were measured. The sample then was warmed to 200 K to recrystallize the partially amorphized H_2CO_3, and to sublime away any H_2O and CO_2 formed, and then recooled to the original temperature. After this annealing cycle, some CO_2 often remained trapped in the H_2CO_3 (trace (c) of Fig. 3). In order to relate only the amount of CO_2 formed to the amount of H_2CO_3 destroyed, at each radiation step we subtracted the band area of any remaining CO_2 in the annealed ice from the area of the CO_2 band recorded after the next irradiation. Table 3 gives the results of these $A(H_2CO_3)$ measurements at 14 and 100 K, corrected for amorphization. The error given in Table 3 is the standard deviation of the linear regression. Because most of the CO_2 product immediately sublimed away upon formation at 200 K, no band strengths were determined at that temperature. Note that the measurements in Table 3 are based on $A(CO_2) = 7.6 \times 10^{-17}$ cm molec^{-1} (Gerakines et al., 1995), and that no decomposition of H_2CO_3 into CO appeared to occur. A few experiments with $H_2{}^{13}CO_3$ were conducted to verify that all of the CO_2 formation observed in our work was due to the proton irradiation, and not from leaks in the vacuum system. No such contamination was detected in any experiment.

3.4. Radiation yield of H_2CO_3

The radiation-chemical yield, denoted G, of a substance is the number of molecules produced by absorption of 100 eV. Previously-reported values for $G(H_2CO_3)$ from $H_2O + CO_2$ (1:1) ices at 14 K were 0.028, 0.030, and 0.02 for MeV protons and UV photons (Gerakines et al., 2000), and for 10 keV electrons from $H_2O + CO_2$ (2:1) ices at 90 K (Hand et al., 2007), respectively. These values were based on the growth of H_2CO_3 IR bands as a function of radiation dose, and represent the formation of H_2CO_3 within an amorphous ice mixture dominated by H_2O and CO_2. We repeated this type of experiment by irradiating $H_2O + CO_2$ (1:1) at 14 K and 50 K in small steps, the 1500 cm^{-1} band's area being measured after each irradiation. The column density of H_2CO_3 was calculated from Eq. (1) using our new band strength for crystalline H_2CO_3. From these experiments we found, $G = 0.11$ and 0.12 for H_2CO_3 formation at 14 K and 50 K, respectively.

As a check on this result, we proton-irradiated an $H_2O + CO_2$ (1:1) mixture at 14 K to a dose of about 10 eV molec^{-1}. We then warmed the sample, as already described, to 240 K followed by recooling to 14 K. Several IR bands of the resulting crystalline H_2CO_3 were integrated and used, with the appropriate A values, to calculate H_2CO_3 column densities. From these results, and the absorbed energy column density (eV cm^{-2}), we found $G(H_2CO_3) = 0.22$, averaged over five different 14 K experiments. The agreement of G values between the two methods is reasonable given the fact that crystalline-phase H_2CO_3 band strengths were used for both calculations, and that some carbonic acid may have formed on warming the irradiated ice. All of our G values for H_2CO_3 formation are compared with published values in Table 4.

Table 3
IR band positions and strengths (A) for H_2CO_3 at 14 and 100 K.

Band position		A (10^{-17} cm molec^{-1})			
Wavenumber (cm^{-1})	Wavelength (μm)	14 K	100 K	18 K[a]	185 K[b]
2749 + 2833	3.634 + 3.530	5.3 ± 1.9	3.3 ± 0.9	9.8	–
2618	3.820	7.5 ± 3.4	7.2 ± 1.7	16.0	–
1695	5.900	10.8 ± 4.4	14.8 ± 3.3	11	35
1503	6.653	5.2 ± 2.1	9.1 ± 1.8	6.5	11
1303	7.675	8.5 ± 2.9	12.3 ± 1.2	10	12.6
1038	9.634	0.15 ± 0.04	0.17 ± 0.05	0.14	–
875	11.43	4.5 ± 0.5	3.7 ± 0.9	5.6	–

[a] From 18 K photodissociation of H_2CO_3 (Gerakines et al., 2000).
[b] From 185 K implantation of H^+ into CO_2 ice to form H_2CO_3 (Garozzo et al., 2008).

Table 4
Radiation chemical yields (G) of H_2CO_3.

Phase and temperature	Yield (G) Number of H_2CO_3 molecules formed or destroyed per 100 eV absorbed			
	This work	Gerakines et al. (2000)		Hand et al. (2007)
	G_{p+}	G_{p+}	G_{uv}	G_{e^-}
Formation				
Crystalline	0.22 ± 0.03	–	–	–
Amorphous[a]				
~10 K	0.11 ± 0.003	0.028 ± 0.024	0.030 ± 0.016	–
50 K	0.12	–	–	–
90 K	–	–	–	0.020
Destruction				
Crystalline				
10 K	−1.3 ± 0.09	−4.2 ± 0.3	$\sigma_{uv} = 1.3 \pm 0.3 \times 10^{-18}$ cm^2	–
100 K	−1.2 ± 0.11	–	–	$\sigma_{e^-} \sim 10^{-16}$ cm^2
200 K	−1.8 ± 0.05	–	–	–

[a] H_2CO_3 was formed in an amorphous ice made from H_2O and CO_2 (1:1). In the last column, a mixture of $H_2O + CO_2$ (2:1) was used by Hand et al. (2007).

We also have observed H_2CO_3 formation during irradiations of $H_2O + CO_2$ ices at temperatures as high as 120 K. However, those results have not yet been quantified and are left for a future paper.

3.5. Vapor pressures and thermal destruction

The vapor pressure of H_2CO_3 was determined by measuring the rate of decrease of the band areas of crystalline H_2CO_3 due to sublimation while maintaining the ice in a vacuum system at a specific temperature (see Khanna et al., 1990). A non-radiation technique was first used to make H_2CO_3 from an acid–base reaction between HBr and $KHCO_3$, as described in Section 2. Fig. 5 shows the similarity between the spectra of radiolytically- and chemically-formed H_2CO_3. The chemically-formed H_2CO_3 also contains some KBr (a side product) and this may account for the 8–18 cm^{-1} shift of some bands with respect to their positions in the radiation-formed H_2CO_3.

Fig. 6 shows the decrease in the normalized average areas for the 1300 and 1500 cm^{-1} bands of H_2CO_3 as a function of time at five different temperatures. Each decrease is related to a change in column density, the number of molecules per cm^2 leaving the ice surface as a function of time. To determine column densities we used A values measured at 100 K. The 185 K A-value data from Garozzo et al. (2008) were not used since their A(1695 cm^{-1}) value is quite large, perhaps because the H_2CO_3 may still contain trapped H_2O. The slopes of similar non-normalized plots gave the sublimation fluxes (molec m^{-2} s^{-1}) at each temperature. Eq. (4) then was used to calculate the vapor pressure, p:

$$\text{Sublimation flux} = p/(2\pi mkT)^{1/2} \quad (4)$$

In Eq. (4), m is the mass of an H_2CO_3 molecule, k is the Boltzmann constant, and T is the absolute temperature, giving a vapor pressure in N m^{-2}, which was converted to units of bar. A plot of the calculated vapor pressure from 238 to 256 K is shown in Fig. 7a. The same data is graphed in Fig. 7b as ln(p) versus 1/T, from which the slope gives the enthalpy of sublimation as $\Delta H_{sub} = 71 \pm 9$ kJ mol^{-1}.

3.6. Chemical destruction

In addition to measurements of both the sublimation and the radiolytic destruction of solid H_2CO_3, we also have observed H_2CO_3 loss by chemical reaction. Previously, we found that ammonia (NH_3) hinders H_2CO_3 formation in irradiated solid-phase $H_2O + CO_2 + NH_3$ mixtures (Gerakines et al., 2000). In separate experiments, we now have irradiated layered ices consisting of a mixture of solid $H_2O + CO_2$ over a layer of NH_3, both ices being formed at ~10 K (Fig. 8). Subsequent irradiation produced H_2CO_3 in the upper layer, as already described in this paper, with the

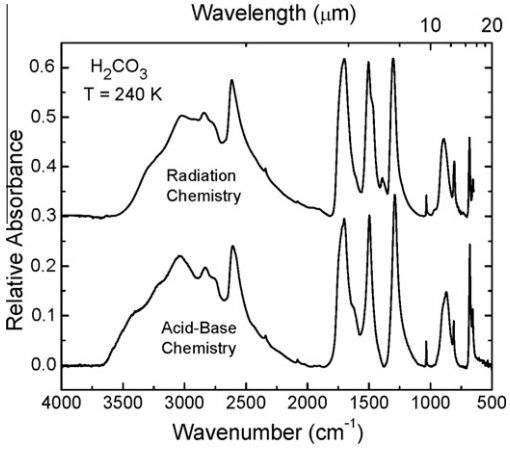

Fig. 5. A comparison of the IR spectra of H_2CO_3 formed by the irradiation of an $H_2O + CO_2$ (1:1) ice and the acid–base reaction of warmed HBr + $KHCO_3$. The upper spectrum was taken with the reflection method described in the text, while the lower spectrum was recorded in a conventional transmission mode.

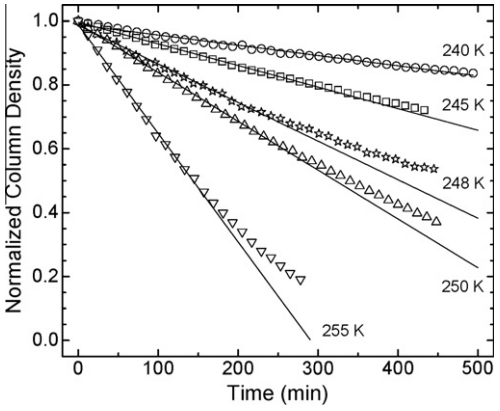

Fig. 6. Normalized areas (averaged) of the 1300 and 1500 cm^{-1} bands of H_2CO_3 plotted as a function of time for five different temperatures. Each point is from the average area of the IR bands at 1300 and 1500 cm^{-1}. For each set of points fitted, $r^2 > 0.99$.

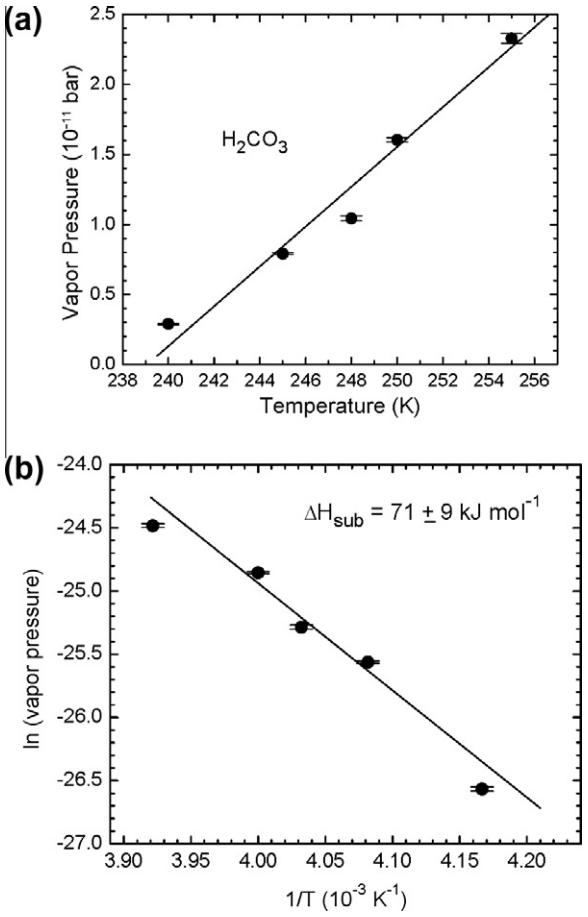

Fig. 7. The vapor pressures of H_2CO_3 at five temperatures are shown in Fig. 7a. A line is drawn to guide the eye. In Fig. 7b, the slope of the regression line (r^2 = 0.944) gives the heat of sublimation, ΔH_{sub} = 71 ± 9 kJ mol^{-1}.

underlying NH_3 ice experiencing only minimal IR-detectable changes. During warming, NH_3 diffuses upward through the irradiated $H_2O + CO_2$ layer containing H_2CO_3. The resulting acid–base reaction and the eventual loss of any remaining NH_3 with continued warming produce the spectrum shown in Fig. 8 (250 K). The upper trace in Fig. 8 is a room-temperature reference spectrum of ammonium carbonate, $(NH_4)_2CO_3$. The match between the two spectra is very close, although small contributions from ammonium bicarbonate (NH_4HCO_3) and even ammonium carbamate ($NH_2CO_2NH_4$) cannot be completely ruled out. (For additional experimental details, and an earlier, now-discarded interpretation of Fig. 8, see Khanna and Moore, 1999). The overall impression of Fig. 8 is that of essentially 100% completion for the following reaction:

$$H_2CO_3 + 2NH_3 \rightarrow (NH_4)_2CO_3 \quad (5)$$

To the best of our knowledge, Fig. 8 is the first published evidence for any reaction of solid H_2CO_3 since its discovery (Moore and Khanna, 1991). In fact, had this acid–base reaction *not* proceeded in the manner just described, it would have cast considerable doubt on the H_2CO_3 spectral assignment.

4. Discussion and astrophysical implications

The results presented here, and in the earlier papers already cited, show that carbonic acid is readily synthesized by both ionizing radiation and vacuum-UV light acting on frozen $H_2O + CO_2$ ice mixtures. After formation, H_2CO_3 can survive on a planetary surface to

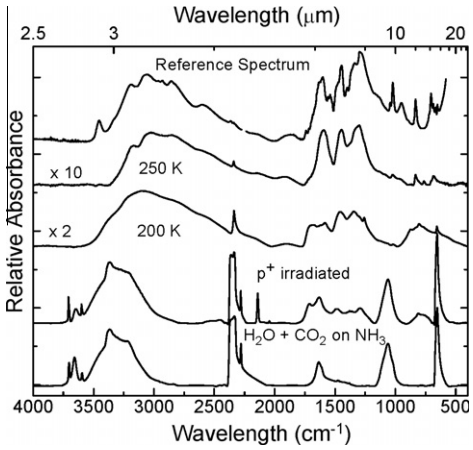

Fig. 8. From bottom to top, the IR spectrum of a mixture of H_2O and CO_2 deposited on top of a layer of NH_3 at 20 K, that same ice after proton irradiation, the irradiated ice warmed to 200 and 250 K, and a reference spectrum of room-temperature ammonium carbonate, $(NH_4)_2CO_3$. The spectra at 200 and 250 K have been expanded vertically by factors of about 2 and 10, respectively.

Table 5
Radiolytic half-lives of crystalline H_2CO_3, corrected for amorphization[a].

Environment	Depth (μm)	Volume dose rate (eV molec^{-1} s^{-1})	Half-life
Laboratory	1.0	1.3×10^{-3}	2.4 h
Europa[b]	100	1.0×10^{-8}	35 years
Callisto[b]	100	2.5×10^{-11}	1.4×10^4 years

[a] Based on the 100-K destruction rate measured in our laboratory.
[b] Volume dose rates for Europa and Callisto from Cooper et al. (2001).

the extent that the molecule is protected from warming and from reactions with NH_3 and other bases. In some cases, radiation environments are sufficiently well known so that our data (Fig. 4) can be used to estimate life-times. Table 5 shows the results of such a calculation, giving a half-life for carbonic acid at 100 K on both Europa and Callisto.

The spectra we have recorded, such as in Fig. 1, illustrate the differences between carbonic acid in an amorphous matrix and pure crystalline H_2CO_3. On warming from 14 to 240 K (traces (b) and (c) of Fig. 1), some peaks shift, some bands narrow, and some

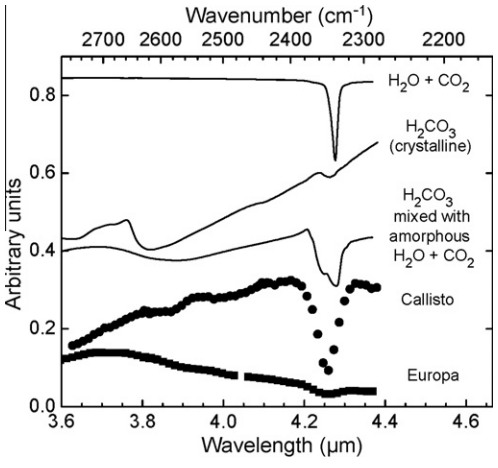

Fig. 9. The IR reflection spectra of Europa and Callisto compared to spectra of an unirradiated $H_2O + CO_2$ mixture at 140 K, crystalline H_2CO_3 at 140 K, and H_2CO_3 mixed with H_2O and CO_2 at 150 K. The H_2CO_3 absorbance spectra were inverted and arbitrarily scaled for this comparison. Callisto's infrared feature at 3.880 μm (2577 cm^{-1}) is matched best by an IR band of H_2CO_3 trapped in the amorphous $H_2O + CO_2$ mixture.

Table 6
Selected thermodynamic properties of H_2CO_3, H_2O, and CO_2.

Ice	Vapor pressures (bar)				Heats of sublimation, ΔH (kJ mol^{-1})
	240 K	245 K	250 K	255 K	
H_2CO_3[a]	$2.90 \pm 0.05 \times 10^{-12}$	$7.92 \pm 0.07 \times 10^{-12}$	$1.60 \pm 0.01 \times 10^{-11}$	$2.33 \pm 0.03 \times 10^{-11}$	71 ± 9
H_2O[b]	2.73×10^{-4}	4.60×10^{-4}	7.60×10^{-4}	1.23×10^{-3}	51.1
CO_2[c]	12.8	15.2	17.9	20.9	25.2

[a] Values for H_2CO_3 are from Fig. 7a and b.
[b] The data for H_2O–ice are from Murphy and Koop (2005).
[c] Vapor pressures for CO_2 are from Stull (1947) while the heat of sublimation is from Giauque and Egan (1937).

splitting is observed. As an example, the broad, weak band near 2555 cm^{-1} (3.914 μm) sharpens considerably and moves to 2612 cm^{-1} (3.828 μm) on warming to 240 K. Fig. 2 shows that this same feature then displays small, reversible shifts in position as the temperature of the carbonic acid is changed. The importance of documenting such spectral variations is demonstrated by Fig. 9, which overlays this same OH stretching feature of carbonic acid on reflectance spectra of Callisto and Europa. The spectrum of pure crystalline H_2CO_3 at 140 K is shown as is one in which carbonic acid is trapped in an amorphous ice mixture at 150 K. For comparison, a spectrum of $H_2O + CO_2$ (7:1) at 140 K is shown. It is seen that the CO_2 band near 4.26-μm on Callisto and Europa is shifted to smaller wavelengths compared to laboratory-measured CO_2, indicating that CO_2 may be complexed at the molecular level with other materials on the satellite surfaces (e.g., Hibbitts and Szanyi, 2007, and references therein). Comparing the band shapes and positions for crystalline-phase pure H_2CO_3 and for H_2CO_3 trapped in amorphous $H_2O + CO_2$ ice, the weak ~3.87-μm Callisto feature is seen to be better fit with the amorphous ice. Any similar feature on Europa is within the noise of the data as demonstrated in Fig. 9. See Johnson et al. (2004) for a suggestion of H_2CO_3 as a possible candidate molecule for Callisto. Additional details on the shifts and intensity changes of H_2CO_3 features can be found in Winkel et al. (2007).

Our analysis of data from irradiated H_2CO_3 considers both radiation-induced chemistry and radiation-induced amorphization. Separating these effects is important because measurements of both H_2CO_3 loss and CO_2 growth are needed for an accurate determination of intrinsic IR band strengths of carbonic acid. Along these lines, the band strengths we report in Table 3 are significantly different (>50%) from some of the older, uncorrected values.

In this paper we have presented data on the destruction of H_2CO_3 at 14, 100, and 200 K, with corrections made for amorphization. The decrease in column density (molec cm^{-2}) of H_2CO_3 plotted as a function of deposited energy density (eV cm^{-2}) was used to calculate $G(-H_2CO_3)$, and values are listed in Table 4. Our destruction measurements, based on the 100 K data, can be converted into radiolytic half-lives on Europa and Callisto, and these are given in Table 5.

We observed that the H_2CO_3 abundance increased on irradiating an amorphous $H_2O + CO_2$ mixture, and eventually reached a plateau, as also reported by Hand et al. (2007). In our experiments the plateau was met after about 6×10^{19} eV cm^{-2} was delivered to the sample, and corresponded to equal rates of formation and destruction for H_2CO_3. At that point ~5% of the CO_2 had been used and of that ~40% ended up in H_2CO_3. The remainder of the carbon from CO_2 was converted to CO and a small trace of CO_3. A similar process on Callisto could result in ~2% H_2CO_3 relative to CO_2.

Table 6 summarizes our vapor pressures for H_2CO_3 and, for comparison, those of frozen H_2O and CO_2 at the same temperatures. It is seen that the vapor pressures for H_2CO_3 are eight orders of magnitude smaller than those of H_2O–ice, and about eleven orders of magnitude smaller than those of CO_2. Therefore, on warmed Solar System surfaces, both CO_2 and H_2O could vaporize leaving behind pure H_2CO_3 for temperatures at or above 170 K. Once in this freeze-dried state, H_2CO_3 would be susceptible to energetic destruction, but otherwise would be fairly stable in a vacuum environment to temperatures as high as ~200 K.

We also have determined, for the first time, the heat of sublimation of H_2CO_3. The value of 71 ± 9 kJ mol^{-1} is large compared to those for H_2O (51.1 kJ mol^{-1}) and CO_2 (25.2 kJ mol^{-1}), which will assist H_2CO_3 in remaining on planetary surfaces after the sublimation of the other two molecules. For comparison to other carboxylic acids, ΔH_{sub} is 62.5 kJ mol^{-1} for formic acid (HCOOH) and 67.9 kJ mol^{-1} for acetic acid (CH_3COOH). See Calis-Van Ginkel et al. (1978).

Having discussed our results, it is appropriate to point out some limitations and possible future work. Two sources of error in Table 1 are the unknown density and radiation stopping power of a 1:1 $H_2O + CO_2$ ice. Our approach was simply to assume these quantities to be an average of the values of the individual components. A direct measurement, particularly of the density, is desirable.

The H_2CO_3 formation we report is for this molecule generated in an amorphous mixture of $H_2O + CO_2$ (1:1). However, to quantify carbonic acid production we were forced to use our *A* values for *crystalline* H_2CO_3. The reason for this is that neither of the synthetic techniques we used to prepare H_2CO_3 resulted in the pure amorphous material. To our knowledge, pure amorphous H_2CO_3 has not yet been made and so no spectra or band strengths are available. A related point concerns the purity of the carbonic acid in our vapor pressure measurements. The acid–base reaction used to make H_2CO_3 gave KBr as a by-product. We do not expect this to influence the vapor pressures of Fig. 7a, but a check with H_2CO_3 made by a different method is desirable.

We also note that our vapor pressure work was done with an IR spectrometer operating in a conventional transmission mode, while measurements of radiolytic destruction utilized reflection spectroscopy. The spectra in the two cases were essentially identical, as seen in Fig. 5.

Finally, the data we have presented here may well have terrestrial applications. Tossell (2009) has suggested solid-phase H_2CO_3 as a candidate for sequestration of atmospheric CO_2, and specifically mentioned the need for measurements of carbonic acid's properties. Among the desired data are carbonic acid's heat of sublimation and vapor pressures, which we report in this paper.

Acknowledgments

The authors acknowledge support through the Goddard Center for Astrobiology, and NASA's Planetary Atmospheres, Outer Planets, and Planetary Geology and Geophysics programs. Zan Peeters also was supported through NASA Grant NNG05GL46G to Catholic University of America. Ariel Lewis worked as a summer researcher at the Goddard Center for Astrobiology. Steve Brown, Tom Ward, and Eugene Gerashchenko, members of the Radiation Laboratory at NASA Goddard, are thanked for operation of the Van de Graaff accelerator. Paul Cooper (George Mason University) is acknowledged for construction of equipment and preliminary vapor

pressure measurements. Robert Carlson (JPL) is thanked for providing the Callisto and Europa data used in Fig. 9.

References

Brown, R.H., and 24 colleagues, 2006. Composition and physical properties of Enceladus' surface. Science 311, 1425–1428.

Brucato, J.R., Palumbo, M.E., Strazzulla, G., 1997. H_2CO_3 by ion implantation in water/carbon dioxide ice mixtures. Icarus 125, 135–144.

Calis-Van Ginkel, C.H.D., Calis, G.H.M., Timmermans, C.W.M., DeKruif, C.G., Oonk, H.A.J., 1978. Enthalpies of sublimation and dimerization in vapor-phase of formic, acetic, propanoic and butanoic acids. J. Chem. Thermodyn. 10, 1083–1088.

Clark, R.N., and 11 colleagues, 2008. Compositional mapping of Saturn's satellite Dione with Cassini VIMS and implications of dark material in the Saturn system. Icarus 193, 372–386.

Cooper, J.F., Johnson, R.E., Mauk, B.H., Garrett, H.B., Gehrels, N., 2001. Energetic ion and electron irradiation of the ice Galilean satellites. Icarus 149, 133–159.

DelloRusso, N., Khanna, R.K., Moore, M.H., 1993. Identification and yield of H_2CO_3 and formaldehyde in irradiated ices. J. Geophys. Res. E 98, 5505–5510.

d'Hendecourt, L.B., Allamandola, L.J., 1986. Time dependent chemistry in dense molecular clouds. III – Infrared band cross sections of molecules in the solid state at 10 K. Astron. Astrophys. Suppl. Ser. 64, 453–467.

Filacchione, G., and 28 colleagues, 2007. Saturn's icy satellites investigated by Cassini-VIMS. I. Full-disk properties: 350–5100 nm reflectance spectra and phase curves. Icarus 186, 259–290.

Garozzo, M., Fulvio, D., Gomis, O., Palumbo, M.E., Strazzulla, G., 2008. H-implantation in SO_2 and CO_2 ices. Planet. Space Sci. 56, 1300–1308.

Gerakines, P.A., Schutte, W.A., Greenberg, J.M., van Dishoeck, E.F., 1995. The infrared band strengths of H_2O, CO and CO_2 in laboratory simulations of astrophysical ice mixtures. Astron. Astrophys. 296, 810–818.

Gerakines, P.A., Moore, M.H., Hudson, R.L., 2000. Carbonic acid production in H_2O:CO_2 ices: UV photolysis vs. proton bombardment. Astron. Astrophys. 357, 793–800.

Giauque, W.F., Egan, C.J., 1937. Carbon dioxide. The heat capacity and vapor pressure of the solid. The heat of sublimation. Thermodynamic and spectroscopic values of the entropy. J. Chem. Phys. 5, 45–54.

Grundy, W.M., Young, L.A., 2004. Near-infrared spectral monitoring of Triton with IRTF/SpeX, I: Establishing a baseline for rotational variability. Icarus 172, 455–465.

Grundy, W.M., Young, L.A., Spencer, J.R., Johnson, R.E., Young, E.F., Buie, M.W., 2006. Distributions of H_2O and CO_2 ices on Ariel, Umbriel, Titania, and Oberon from IRTF/SpeX observations. Icarus 184, 543–555.

Hage, W., Hallbrucker, A., Mayer, E., 1993. Carbonic acid: Synthesis by protonation of bicarbonate and FTIR spectroscopic characterization via a new cryogenic technique. J. Am. Chem. Soc. 115, 8427–8431.

Hand, K.P., Carlson, R.W., Chyba, C.F., 2007. Energy, chemical disequilibrium, and geological constraints on Europa. Astrobiology 7, 1006–1022.

Hansen, G.B., McCord, T.B., 2008. Widespread CO_2 and other non-ice compounds on the anti-jovian and trailing sides of Europa from Galileo/NIMS observations. Geophys. Res. Lett. 35, L01202.

Hibbitts, C.A., Szanyi, J., 2007. Physisorption of CO_2 on non-ice materials relevant to icy satellites. Icarus 191, 371–380.

Hibbitts, C.A., McCord, T.B., Hansen, G.B., 2000. Distributions of CO_2 and SO_2 on the surface of Callisto. J. Geophys. Res. – Planets 105, 22541–22558.

Hibbitts, C.A., Pappalardo, R.T., Hansen, G.B., McCord, T.B., 2003. Carbon dioxide on Ganymede. J. Geophys. Res. – Planets 108. ID: 5036.

Hudson, R.L., Moore, M.H., 2004. Reactions of nitriles in ices relevant to Titan, comets, and the interstellar medium: Formation of cyanate ion, ketenimines, and isonitriles. Icarus 172, 466–478.

Johnson, R.E., Carlson, R.W., Cooper, J.F., Paranicas, C., Moore, M.H., Wong, M.C., 2004. Radiation effects on the surfaces of the Galilean satellites. In: Bagenal, F., Dowling, T.E., McKinnon, W.B. (Eds.), Jupiter. The Planet, Satellites, and Magnetosphere, vol. 1. Cambridge University Press, Cambridge, UK, pp. 485–512.

Khanna, R.K., Moore, M.H., 1999. Carbamic acid: Molecular structure and IR spectra. Spectrochim. Acta 55A, 961–967.

Khanna, R.K., Allen Jr, J.E., Masterson, C.M., Zhao, G., 1990. Thin-film infrared spectroscopic method for low-temperature vapor pressure measurements. J. Phys. Chem. 94, 440–442.

Loerting, T., Tautermann, C., Kroemer, R.T., Kohl, I., Hallbrucker, A., Mayer, E., Liedl, K.R., 2000. On the surprising kinetic stability of carbonic acid (H_2CO_3). Angew. Chem. Int. Ed. 39, 892–894.

Moore, M.H., Hudson, R.L., 1998. Infrared study of ion-irradiated water–ice mixtures with hydrocarbons relevant to comets. Icarus 135, 518–527.

Moore, M.H., Khanna, R.K., 1991. Infrared and mass spectral studies of proton irradiated $H_2O + CO_2$ ice: Evidence for H_2CO_3. Spectrochim. Acta 47A, 255–262.

Moore, M.H., Khanna, R.K., Donn, B., 1991. Studies of proton irradiated $H_2O + CO_2$ and H_2O + CO ices and analysis of synthesized molecules. J. Geophys. Res. E 96, 17541–17545.

Moore, M.H., Hudson, R.L., Carlson, R.W., 2007. The radiolysis of SO_2 and H_2S in water ice: Implications for the icy jovian satellites. Icarus 189, 409–423.

Murphy, D.M., Koop, T., 2005. Review of the vapour pressures of ice and supercooled water for atmospheric applications. Quart. J. R. Meteorol. Soc. 131, 1539–1565.

Stull, D.R., 1947. Vapor pressure of pure substances. Organic compounds. Ind. Eng. Chem. 39, 517–540.

Tossell, J.A., 2009. H_2CO_3(s): A new candidate for CO_2 capture and sequestration. Environ. Sci. Technol. 43, 2575–2580.

Winkel, K., Hage, W., Loerting, T., Price, S., Mayer, E., 2007. Carbonic acid: From polyamorphism to polymorphism. J. Am. Chem. Soc. 129, 13863–13871.

Wu, C.Y.R., Judge, D.L., Cheng, B., Yih, T., Lee, C.S., Ip, W.H., 2003. Extreme ultraviolet photolysis of CO_2–H_2O mixed ices at 10 K. J. Geophys. Res. – Planets 108, 13-1–13-8.

Zheng, W., Kaiser, R.I., 2007. On the formation of carbonic acid (H_2CO_3) in Solar System ices. Chem. Phys. Lett. 450, 55–60.

Ziegler, J.P., Biersack, J.P., Littmark, U., 1985. The Stopping and Range of Ions in Solids. Pergamon, New York. <http://www.srim.org>.